Journal of Materials Processing Technology 140 (2003) 30–35

Journal of Materials Processing Technology

www.elsevier.com/locate/jmatprotec

Simulation of ultrasonic-vibration drawing using the finite element method (FEM)

Masahiro Hayashi [a], Masahiko Jin [a,*], Sutasn Thipprakmas [a], Masao Murakawa [a], Jung-Chung Hung [b], Yu-Chung Tsai [b], Ching-Hua Hung [b]

[a] *Department of Mechanical Engineering, Nippon Institute of Technology, 4-1 Gakuendai, Miyashiro-machi Minamisaitama-gun, Saitama 345-8501, Japan*

[b] *1001 Ta Hsueh Road, Heinchu 300, Taiwan, ROC*

Abstract

In ultrasonic-vibration drawing, wires are drawn while ultrasonic vibration is applied to a drawing die. Prior studies provide experimental proof that ultrasonic-vibration drawing reduces drawing resistance, improves lubrication and prevents wire breakage. In the future, ultrasonic-vibration drawing is expected to contribute to the drawing of difficult-to-draw materials and operations, such as shaped wires, ultrafine wires, and the wire drawing operation in semidry or dry condition. However, a detailed analysis and understanding of the mechanism of improvement is not possible on the basis of conventional experimental observations because the ultrasonic-vibration processing phenomenon occurs at high speed. Therefore, we attempted to understand the processing mechanism of ultrasonic-vibration drawing using the finite element method (FEM). ABAQUS was used for the FEM. Drawing force and stress–strain distributions in drawn wires were analyzed. From these studies, we quantitatively clarified the mechanism of improved drawing characteristics, such as decreased drawing force.

Keywords: Wire drawing; Ultrasonic vibration; Finite element method (FEM); Drawing force

1. Introduction

In recent years, the drawing of difficult-to-draw materials, such as various titanium alloys and inter-metallic compounds, or difficult-to-draw operations, such as processing of shaped wires used for glass frames and ultrafine wires for use in wire bonding are often required [1,2]. On the other hand, from the viewpoint of the reduction of environmental burden, the use of chlorine-free lubricant in the process, furthermore, semidry or dry process has been demanded [3].

Ultrasonic-vibration drawing has been considered as a means of accommodating these high-level drawing processes. This drawing method involves the application of ultrasonic vibration to either the axial or radial direction of the die during drawing. To date, it has been proven that this drawing method contributes to the improvement of lubricant conditions and the decrease in drawing force [4]. It is expected that the ultrasonic-vibration drawing method will be viewed as an effective means of resolving the issues discussed above.

Several studies have been conducted on this subject. Mori and Inoue [5] carried out the study to fabricate fine wires by the use of the axial direction ultrasonic-vibration drawing method. Sansome [6] studied on tube drawing by the radial direction ultrasonic-vibration drawing method. Murakawa et al. [7] realized chlorine-free skin-pass drawing of stainless steel wires by the application of the radial direction ultrasonic-vibration drawing method.

Some studies were attempted to analyze the mechanism of improved drawing performances, such as reduced drawing force and improved lubrication characteristics [8,9]. However, detailed and quantitative experimental analyses have not been performed because of the difficulty of real-time measurements of drawing phenomena during the application of ultrasonic vibration.

To overcome this difficulty, we carried out a quantitative study of the mechanism of improved drawing characteristics in ultrasonic-vibration drawing using FEM analysis. We used a program (ABAQUS) for the FEM and analyzed the drawing force and the stress and strain distributions in the wire.

* Corresponding author. Tel.: +81-480-33-7614; fax: +81-480-33-7645.
E-mail address: jin@nit.ac.jp (M. Jin).

0924-0136/$ – see front matter © 2003 Elsevier B.V. All rights reserved.
doi:10.1016/S0924-0136(03)00699-X

As a result of the study, it has become possible to quantitatively understand the mechanism of improved drawing characteristics such as reduced drawing force.

2. Results of experimental evaluation of relationship between drawing speed and drawing force in past study [8]

Fig. 1 shows the ultrasonic-vibration wire drawing mechanisms for (1) axial (ultrasonic) vibration drawing (AUD) and (2) radial (ultrasonic) vibration drawing (RUD), and the relationship between drawing speed and drawing force based on data that were obtained experimentally for conventional drawing (CD), AUD and RUD. In these experiments, the ultrasonic-vibration frequency (f) was 15 kHz, the amplitude (a) was 1 μm and the drawn wire diameter (d_w) was 6.0 mm. The material used was pure aluminum wire, A1070-H. The reduction ratio R was 6.6%.

The results indicate that drawing force was independent of drawing speed in the case of CD; i.e. it was constant at 620 N. On the other hand, the drawing force increased with drawing speed in the case of AUD. The drawing force is equal to that obtained for CD under the critical drawing speed condition (i.e. $V_c = 2\pi af = 93.6$ mm/s) at which the maximum ultrasonic-vibration speed is roughly equal to the drawing speed. On the other hand, in the case of RUD, the relationship between drawing speed and drawing force is similar to that obtained for AUD. However, the critical drawing speed condition (V_c) is expressed by $V_c = 2\pi af/\tan\alpha$; it was 890.5 mm/s at die half angle of $\alpha = 6^\circ$ in the case of RUD. This is 9.9-fold higher than for AUD.

Generally, speaking, drawing force generated by AUD and RUD ultrasonic-vibration drawing is substantially small compared with that generated by CD. The drawing force reducing effect increases with decreasing drawing speed. Unfortunately, these experimental results do not represent real-time drawing resistance under ultrasonic-vibration conditions. In other words, ultrasonic-vibration frequencies used in drawing apparatus are generally two orders of magnitude higher than the natural frequencies of measurement systems. Therefore, we think that the measured drawing force indicates an average value of actual dynamic drawing force by the ultrasonic-vibration period. The difficulty of real-time measurement of drawing force remains unresolved.

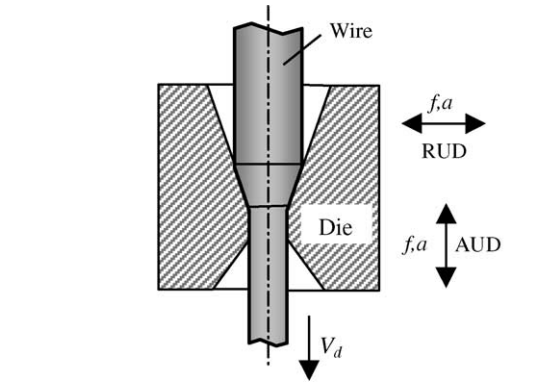

(a) Ultrasonic-vibration wire drawing mechanisms for AUD and RUD

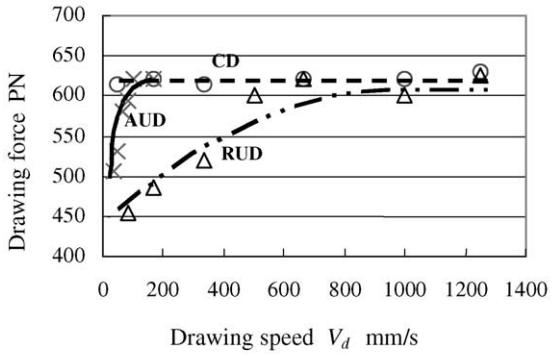

(b) Experimental results of relationship between drawing speed and drawing force

Fig. 1. Ultrasonic-vibration wire drawing mechanisms and relationship between drawing speed and drawing force in CD, AUD and RUD (Section 2).

3. FEM simulation method of ultrasonic-vibration drawing

Fig. 2 shows the FEM analysis model used in this study and Table 1 shows the conditions used in the analysis. "ABAQUS standard", a commercially available analysis code, was used in the analysis. The analysis is based on a

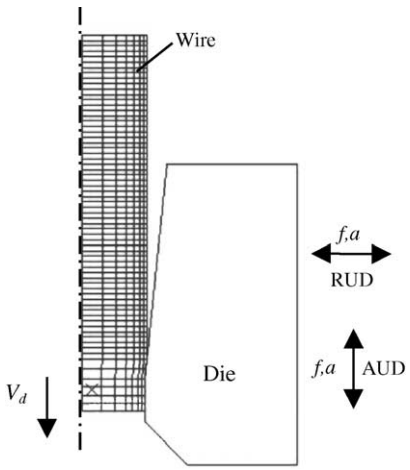

Fig. 2. FEM simulation model of ultrasonic-vibration wire drawing method.

Table 1
FEM simulation conditions

Wire	Elasto-plastic deformable body
Die	Rigid body
Simulation model	Axisymmetric model
FEM program	ABAQUS standard

Table 2
Material properties and drawing conditions

Wire drawing speed (V_d)	30–9000 mm/s
Wire material	Aluminum (A1070-H)
Young's modulus (E)	69 GPa
Yield strength (σ_y)	55.43 MPa
Poisson's ratio (ν)	0.33
Density	3.6 g/cm^3
Die material	Sintered carbide
Density	14.8 g/cm^3
Diameter of wire	Ø 6.0 mm
Diameter of die	Ø 5.8 mm
Reduction (R)	6.6%
Length of wire drawing (L)	16 mm
Friction coefficient (μ)	0.05

Table 3
Ultrasonic-vibration conditions

	Vibration direction	Frequency, f (kHz)	Amplitude, a (0-P) (μm)
CD	None	None	None
AUD	Axial direction	14.9	1, 10
RUD	Radial direction	14.9	1, 10

two-dimensional axial symmetry model. Analyses were performed for CD, AUD and RUD. In the simulation, the wire materials used for drawing were defined as an elasto-plastic body and the die as a rigid body.

Table 2 shows material properties and drawing conditions used in the analysis. The drawing conditions were set on the basis of the above experimental conditions; the diameter of the wire drawn (d_w) was 60 mm and it is pure aluminum, A1070-H. The die diameter (d) was 5.8 mm. The reduction ratio (R) was 6.6%.

Table 3 shows vibration conditions in ultrasonic-vibration drawing. The axial and radial vibration frequencies were $f = 14.9$ kHz. The amplitude was set to $a = 1$ and 10 μm.

4. Results of analysis and discussion

4.1. Relationship between drawing speed and drawing force

Fig. 3 shows the result of calculation of drawing force (P) at two different levels of drawing speed for the case of CD. In each figure, the abscissa and ordinate represent time and drawing force, respectively. The drawing force (P) was constant at approximately 620 N ($\sigma = 23.5$ N/mm^2) regardless of drawing speed (V_d). There was measurement fluctuation within 60–80 N which is considered to be caused by calculation error of FEM analysis.

Next, Fig. 4 shows the results of analysis for AUD, which is similar to the preceding analysis. In these studies, as shown in Fig. 4(a), the drawing force was within the range of 450 N ($\sigma = 17.0$ N/mm^2) to 670 N ($\sigma = 25.4$ N/mm^2) and

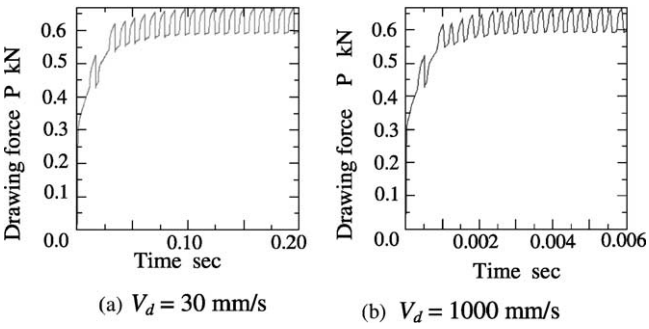

Fig. 3. Drawing force diagrams for CD analyzed by FEM (amplitude 1 μm).

fluctuated at the period of ultrasonic vibration (67 μs) when $V_d = 30$ mm/s, which is below the critical drawing speed. Fig. 4(b) shows details of the fluctuation period for drawing force. When the drawing speed is greater than the critical drawing speed, $V_d = 300$ mm/s, as shown in Fig. 4(c), the drawing force, P, was approximately the same as the value obtained for CD, 620 N ($\sigma = 23.5$ N/mm^2). This means that the drawing force fluctuation caused by ultrasonic vibration was eliminated.

Finally, similar analyses to those above were performed in the case of RUD; Fig. 5 shows the results. As shown in Fig. 5(a), the drawing force fluctuates within the range of 280 N ($\sigma = 10.6$ N/mm^2) to 580 N ($\sigma = 22.0$ N/mm^2) with a period of ultrasonic vibration of 67 μs at $V_d = 30$ mm/s. Next, drawing force P fluctuated within 400 N ($\sigma = 15.1$ N/mm^2) to 620 N ($\sigma = 23.5$ N/mm^2) at $V_d = 300$ mm/s. However, drawing force was almost the same as that observed in the case of CD, i.e. 620 N ($\sigma = 23.5$ N/mm^2) at $V_d = 1000$ mm/s.

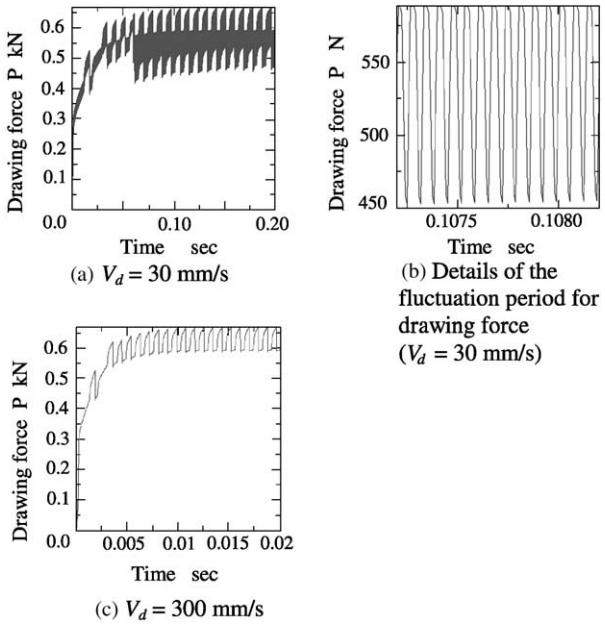

Fig. 4. Drawing force diagrams for AUD analyzed by FEM (amplitude 1 μm).

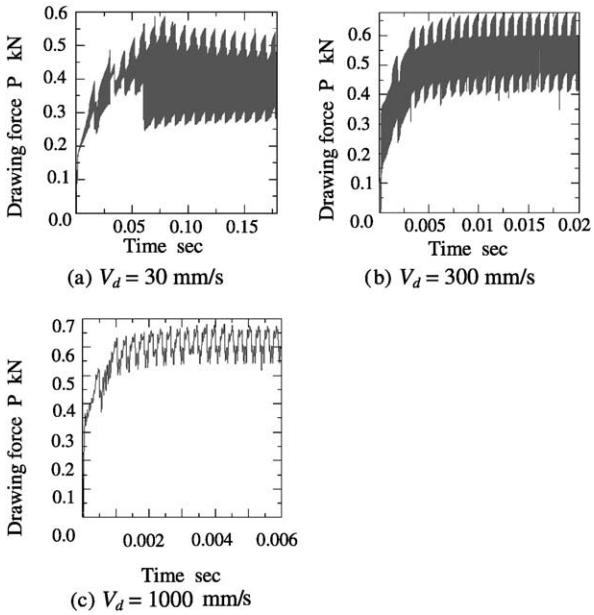

Fig. 5. Drawing force diagrams for RUD analyzed by FEM (amplitude 1 μm).

The above results can be summarized as follows. For both AUD and RUD, the drawing force fluctuated with a period of the die vibration when drawing speed was below the critical drawing speed and the fluctuation amplitude tended to increase with decreasing drawing speed. When drawing speed reaches the critical value, the fluctuation of drawing force disappears; the waveform is essentially the same as that observed in CD analysis.

4.2. Comparison of experimental and analytical results regarding the relationship between drawing speed and drawing force

As described above, drawing force measured by the experiments is considered to be the average value of the actual fluctuating drawing force owing to the ultrasonic vibration. Fig. 6 shows the relationship between drawing speed and

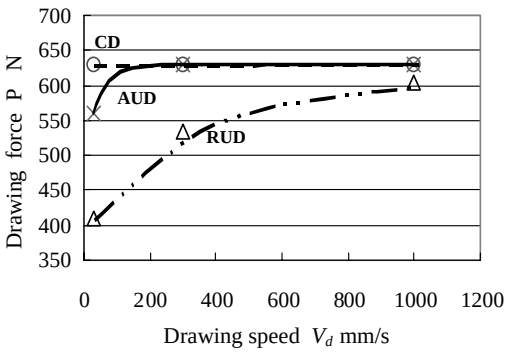

Fig. 6. Relationship between drawing speed and drawing force in CD, AUD and RUD (FEM simulation results).

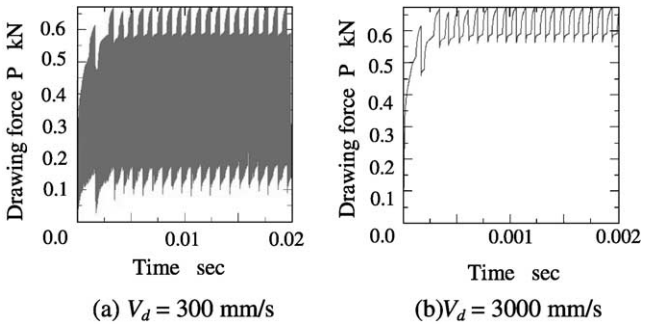

Fig. 7. Drawing force diagrams for AUD (amplitude 10 μm).

drawing force for CD, AUD and RUD. According to FEM analysis, the average drawing force in CD is independent of drawing speed and is essentially the same as that obtained in experiments. Drawing force is constant at 620 N. In the case of AUD, the profile of drawing force changed at the dividing point, which is the critical drawing speed V_d. The critical drawing speed is 93.6 mm/s in the case of AUD. The profile is similar to that obtained for CD when the drawing speed is at the critical speed or higher. On the other hand, the drawing force tended to approach zero with decreasing drawing speed when the drawing speed is lower than the critical speed. The drawing force tendencies for AUD and RUD were almost the same. However, the critical drawing speed of RUD is approximately 10-fold that of AUD.

In other words, the FEM analysis describing the relationship between drawing speed and drawing force in this study yielded the same results in this study as those obtained by conventional experiments.

4.3. Relationship between amplitude of ultrasonic vibrations and drawing force

According to the critical drawing speed concept, a large drawing force reduction can be obtained by increasing either the frequency or amplitude of ultrasonic vibration. These effects are seen under high-speed drawing conditions and are beneficial in terms of productivity.

Considering the above observations, we performed FEM simulations on drawing force waveforms for the case when the amplitude was set 10 times higher than the previous experiment (i.e. $a = 10$ μm). The reason for analyzing drawing force at high amplitudes is that it is easier to increase amplitude than to increase frequency due to the characteristics of ultrasonic-vibration devices. Furthermore, it is practical to obtain an amplitude (a) of 10 μm at a vibration frequency (f) of 15 kHz.

First, Fig. 7 shows results of drawing force obtained by FEM analysis for two levels of drawing speed for AUD. According to the results, the fluctuation of drawing force due to ultrasonic vibration improved approximately 10-fold compared with the results shown in Fig. 4.

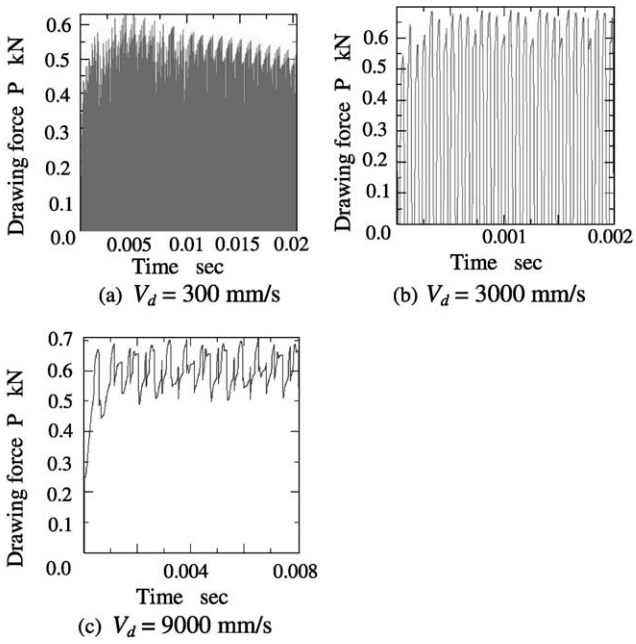

Fig. 8. Drawing force diagrams for RUD analyzed by FEM (amplitude 10 μm).

Next, Fig. 8 shows the results of FEM analysis of drawing force waveform for three levels of drawing speed in the case of RUD. Again, similar to the case of AUD, the fluctuation range of drawing force improved compared with the results shown in Fig. 5. In particular, the lower limit of drawing force was zero at drawing speeds (V_d) of 300 mm/s or less. This means that the die was completely separated from the wire. In other words, the hypothesis that drawing advances while the die and the wire repeat the process of contact and separation in RUD has been proven quantitatively by means of FEM analysis.

Fig. 9 shows the frequency-averaged drawing force for CD, AUD and RUD at an amplitude (a) of 10 μm. Thus, similar to the results discussed above with respect to Fig. 6, the drawing force decreases substantially and approaches zero when the drawing speed is less than or equal to the critical drawing speed for both AUD and RUD. Furthermore, FEM analysis predicted continuation of vibration effects up to the high drawing speed (V_d) of 8900 mm/s for RUD.

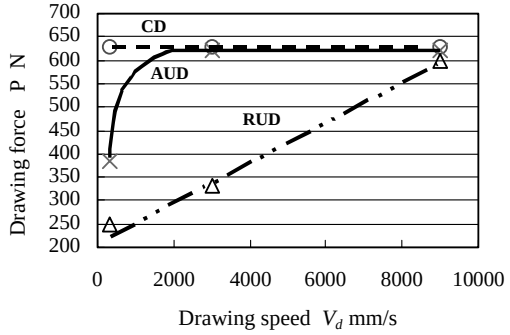

Fig. 9. Relationship between drawing speed and drawing force in CD, AUD and RUD (FEM simulation results).

4.4. Comparison of stress distributions in the wire drawn by the ultrasonic-vibration drawing method

Fig. 10 shows the stress distribution in the wire during drawing by CD, AUD and RUD. Fig. 10(a) shows the von Mises stress distribution for CD. The maximum stress value is found near the surface layer of the die-bearing section and maximum stress value is 146.7 MPa. On the other hand, as

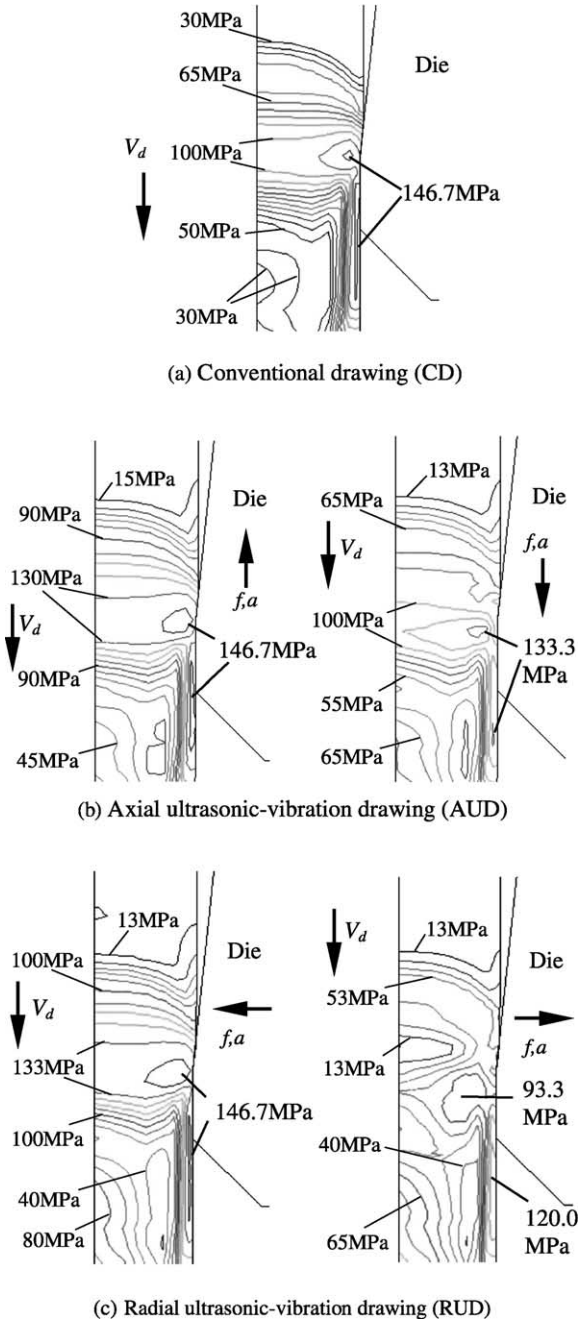

Fig. 10. von Mises stress distribution in the wire during drawing by CD, AUD and RUD (drawing speed 300 mm/s, amplitude 10 μm).

shown in Fig. 10(b), when the vibration direction of the die is opposite to the direction of drawing, the stress distribution was similar to that of CD in the case of AUD. However, when the direction of vibration is in the same direction as drawing, the maximum stress value decreased by approximately 91% compared to CD. As shown in Fig. 10(c), when the vibration of the die is directed to the center of the wire, the stress distribution for RUD is similar to that obtained for CD. On the other hand, when the direction of vibration is in the radial direction of the wire, the maximum stress value decreases substantially by 64%.

In both AUD and RUD, the maximum stress value in wires tended to decrease periodically. FEM analysis showed a tendency for a greater rate of decrease of the maximum stress value at higher amplitudes, in the case of RUD.

On the other hand, FEM analysis was performed on equivalent plastic strain distribution inside a drawn wire. There was no significant difference in equivalent plastic strain among CD, AUD and RUD.

5. Conclusions

We performed simulations using FEM on drawing force and stress–strain distribution of wires drawn by AUD and RUD. The simulations clarified the following points.

(1) For both AUD and RUD, it is possible to quantitatively analyze the drawing force waveform, which changes according to the period of ultrasonic vibration.
(2) The frequency-averaged values of fluctuating drawing force waveforms for AUD and RUD agree closely with results of drawing force measurements in conventional experiments.
(3) The critical drawing speed calculated by FEM analysis essentially agrees with the theoretical value obtained on the basis of the equality of the drawing speed obtained by conventional methods and the speed of vibration under maximum vibration amplitude conditions.
(4) FEM analysis quantitatively clarified the dependence of the reduction of drawing speed on amplitude.
(5) FEM analysis quantitatively revealed changes in stress distribution in wires.

Acknowledgements

This research was conducted as a joint study between Nippon Institute of Technology and Taiwan National Chiao Tung University. The two universities have a partnership as sister universities. We are thankful for the support extended by both universities. We thank Professor Kazuya Yoshida of the School of Engineering, Tokai University, Japan for his assistance with the drawing experiment.

References

[1] S. Norasethasopon, K. Yoshida, Finite-element simulation on wire breakage induced by eccentric inclusion in shaped wire drawing, Proc. School Eng. Tokai Univ. 27 (2002).
[2] K. Yoshida, M. Watanabe, H. Ishikawa, Drawing of Ni–Ti shape-memory alloy fine tubes used in medical tests, J. Mater. Process. Technol. 118 (2001).
[3] K. Seiji, Environmentally friendly lubricating technology in future, J. JSTP 43 (492) (2002) (in Japanese).
[4] L. Li, X. Lang, Wire drawing with ultrasonic vibration, J. Wire Ind. 61 (721) (1994).
[5] E. Mori, M. Inoue, Effects of drawing speed and backward tension application of ultrasonic vibration to metal wire drawing (2nd report). J. JSTP 11 (144) (1970) (in Japanese).
[6] D.H. Sansome, New developments in ultrasonic tube-drawing, Tomorrow Tube (1986).
[7] M. Murakawa, P. Kaewtatip, M. Jin, Skin pass wire drawing of stainless steel with chlorine-free lubricant with the aid of ultrasonic vibration, Trans. NAMRI/SME 29 (2000).
[8] M. Murakawa, M. Jin, The utility of radially and ultrasonically vibrated dies in the wire drawing process, J. Mater. Process. Technol. 113 (2001).
[9] Y. Meng, X. Liu, J. Chen, A dynamic contact model for ultrasonic wire drawing, Proc. ICTMP 1 (1997).